Journal of Advanced Research in Fluid Mechanics and Thermal Sciences

Journal homepage:
https://semarakilmu.com.my/journals/index.php/fluid_mechanics_thermal_sciences/index
ISSN: 2289-7879

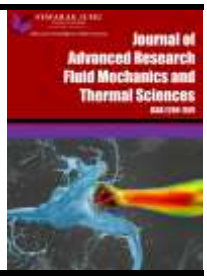

A Numerical Investigation on Boundary Layer Flow of MHD Tangent Hyperbolic Fluid Flow over a Stretching Sheet with Slip Boundary Conditions

Banda Narsimha Reddy[1], Ramya Dodda[2], Borra Shashidar Reddy[3,*]

[1] Department of Mathematics, Anurag University, Venkatapur, Hyderabad, 500088 Telangana, India
[2] Department of Science and Humanities, Pallavi Engineering College, Kuntloor, Hyderabad, 501505 Telangana, India
[3] Department of Mathematics, Sreenidhi Institute of Science and Technology, Ghatkesar, 501301 Telangana, India

ARTICLE INFO

Article history:
Received 16 April 2024
Received in revised form 15 July 2024
Accepted 24 July 2024
Available online 15 August 2024

Keywords:
Thermophoresis; Brownian motion; nanofluid; Keller box method; power-law index; thermal and velocity slip

ABSTRACT

This investigation addresses the flow of hyperbolic tangential magnetohydrodynamic (MHD) fluids across a stretching sheet, discussing its thermophysical properties and observing the boundary conditions for velocity and thermal slip. The mathematical model converts coupled non-linear PDEs to ordinary differential equations with the aid of local similarity variables. In order to fix the derived ordinary differential equations, the Keller box method is utilized. This paper summarizes quantitative and qualitative effects of various flow regulating parameters which modify concentrations, temperatures, and velocities. In addition, the behavior near the stretched sheet is examined by computing the wall friction factor and the local Nusselt number. Both computational and conceptual computations of the wall friction factor and local Nusselt number are compared, and the findings show a strong agreement, giving credibility to the numerical results.

1. Introduction

The analysis of the movement of thick fluids across an elongating surface is very relevant in several engineering applications. This flow phenomenon is essential in multiple industrial processes, such as wire drawing, transferring among the feed rollers and wind-up turns, exposed to heat materials, extrusion-based material manufacturing, techniques for freezing electronic components or metals sheets of paper, plastic sheet drawing, crystal growth, Manufacture of both paper as well as fibres of glass and various other manufacturing procedures. Improving process optimization, product quality, and engineering and manufacturing technology as a whole relies on a firm grasp of viscous fluid dynamics as it pertains to these situations. The cooling process plays a crucial role in defining the final product's qualities when applied to the stretching sheet. The efficiency of the cooling process has a direct impact on the final product's quality, characteristics, and performance is shown by Hady *et al.,* [1]. The investigation of boundary layer flow problems that are axi-symmetric

* *Corresponding author.*
E-mail address: bsreddy_shashi@yahoo.com

https://doi.org/10.37934/arfmts.120.1.122139

and two-dimensional was initiated by Sakiadis [2]. A non-linear stretched sheet was computationally explored for heat transfer and viscous flow by Cortell [3]. The free convective mass and heat transfer in MHD fluid flow over a permeable vertical stretched sheet was studied by Rashidi *et al.,* [4]. Impacts of buoyancy and radioactivity were considered in the study using the homotopy analysis method. Taking into account, the characteristics of chemical reactions and the influence of an electromagnetic field. Rapits and Perdikis [5] looked into the viscous flow across a non-linearly stretching sheet employing shooting technique. Turbulent movement of mixed type across a non-linear stretched sheet by a fluid with micropolarity was studied using the Homotopy evaluation approach is addressed by Hayat *et al.,* [6]. Parametric study of micropolar fluid over a vertical permeable stretching sheet was done by Khan *et al.,* [7].

Fluid flow in magnetohydrodynamics (MHD) with mass and heat transport has been the subject of intense investigation for the past few decades. Such occurrences are common in scientific and technical processes, which is why there has been a rise in research on the subject. Heat exchangers, chemical engineering procedures, nuclear process systems, groundwater systems, electronic cooling, heat loss from pipes, and MHD accelerators are among the significant applications. Understanding and treating MHD fluid flow is crucial in numerous domains due to its vast range of applications. Utilizing the Keller-box technique, Prasad *et al.,* [8] investigated the effect of fluid characteristics on MHD flow and heat transmission across a stretching material. Khan *et al.,* [9] used similarity transforms to study the influence of thermal- diffusion on the stagnation point flow of a nanofluid toward a stretching surface in the vicinity of a magnetic field. Under the consideration of heat and mass, Darcy-Forchheimer relation in convective MHD nanofluid flows limited by non-linear stretching surfaces was solved numerically by Rasool *et al.,* [10]. The influence of thermophoresis and the Soret-Dufour on the mass and heat transfer flow of magnetohydrodynamic non- Newtonian nanofluid across an inclined plate was looked into by Idowu and Falodun [11]. An investigation of a computer model of a magneto hydrodynamic Carreau liquid including gyrotactic microbes was completed by Naz *et al.,* [12]. Uddin *et al.,* [13] examined the Darcian porous medium: magneto-convective boundary layer with slip flow media over a non-isothermal moving permeable plate with non-linear radiation. The Runge-Kutta-Fehlberg numerical method, which is fourth-or fifth-order, was employed in their analysis.

An exceptionally capable method for depicting shear-thinning events is a model of tangential hyperbolic fluids. The capacity of the fluids to maintain a reduced flow rate in the face of increasing shear stress rates is captured by this model. Ketchup, paint, and blood are typical instances of fluids that display this pseudoplastic pattern. Tangent hyperbolic fluids are a good description for non-Newtonian fluids, particularly those exhibiting shear-thinning behavior. To better understand and define the behavior of fluids having pseudoplastic features, the model of tangential hyperbolic fluid hyperbolic fluid has been the subject of a great deal of research in the literature. This research has taken into account a wide range of physical phenomena. This study expands our understanding a non-Newtonian fluid and their practical application in various real-life situations. The magnetohydrodynamic flow through a stretching cylindrical of a hyperbolic tangential fluid has been addressed by Khan *et al.,* [9]. The investigation of the study was carried out using the Keller box approach. In their extensive study, Nadeem and Akbar [14] examined the movement of peristaltic objects of tangent hyperbolic fluid in a uniformly inclined tube. Using the perturbation approach and the homotopy analysis method, they calculated series solutions to the governing equations. Using a tangent hyperbolic nanoliquid of varying thickness, Malik *et al.,* [15] considered magnetohydrodynamic (MHD) stretched flows. Naseer *et al.,* [16] investigated the properties of heat transmission for a tangent hyperbolic fluid across a vertical cylinder that is stretched exponentially. It is important to note that this research is the initial examination of this kind of situation. The authors

used the Runge-Kutta-Fehlberg technique to numerically resolving the resultant problem. The impact of heat production as well as indulging in magnetohydrodynamic hyperbolic tangent fluid movement on an expanded surface is developed by Salahuddin *et al.,* [17]. Furthermore, an analytical and numerical solution for the tangential hyperbolic nanofluid with MHD stagnating region flow across a stretching cylindrical is reported by Salahuddin *et at.,* [18]. Tangent hyperbolic nanofluid flows have been investigated by other authors [19-23].

There are many practical uses for the effects of boundary slip in fluids, like when artificial internal chambers and the heart valves are polished. When information on the thermal slip coefficient is scarce, microscale liquid flow conditions involving velocities and thermal leaps become critical. Many complicated micro-channels and micro-devices fit this description well. Rectangular, trapezoidal, and triangular micro-conduits are examples of typical and easily buildable micro-scale thermal fluid systems the homotopy analysis technique (HAM). Mustafa *et al.,* [24] assessed how peristaltic motion is affected by the impacts of nanofluid slipping in a wall tunnel characteristic. Mukhopadhyay [25] examined the effects of slip on the magnetohydrodynamic (MHD) flow of the boundary layer over an exponential stretching sheet, including suction/blowing and thermal radiation. A numerical study by Malvandi *et al.,* [26] looked at how the unstable stagnant region movement of a nanofluid technology is affected by temperature and velocity slip over a stretching sheet. For a nanofluid passing over a porous stretched sheet, heat transfer and magnetohydrodynamic (MHD) flow through boundary layer characteristics were studied by Ibrahim and Shankar [27]. The work addressed boundary conditions for thermal, solutal, and slip-in-velocity components. Singh *et al.,* [28] applied keller box approach to address micropolar fluid flow through porous wedge with Hall and ion-slip.

For instance, in the cleaning of mechanical heart valves and inner cavities, fluid models with boundary slip play a vital part in healthcare and technical applications. When dealing with coated physical substances that are resistant to adhesion, like bakelite, Navier's slip replaces the no-slip condition. In this case, the slip velocity is related to the local shear stress. But experiments show that normal stress is also a factor in slide velocity. When slip fluid conditions are present, Turkyilmazoglu [29] noticed that the magnetohydrodynamic (MHD) double and triplicate answers for the electrically conductive non-Newtonian slip flow movement across a contracting sheet. When considering the boundary layer flow over a moving plate for the movement of heat, Ellahi *et al.,* [30] looked at the impacts of slip and MHD using particular entropy generation. Through numerical analysis, Reddy *et al.,* [31] investigated the boundary layer Maxwell slip flow nanofluid across an exponential stretched surface under boundary conditions of convection. Featuring the velocity slip model, Aly and Sayed [32] investigated the effect of magnetohydrodynamics and heat radiation on the flow of boundary layer caused by an extensible surface that is in motion: An analysis of four nanofluids in comparison. Williamson nanofluids with porous media have their mass and heat transported through the boundary later, and the influence of velocities and thermal slips on this process is described by Reddy *et al.,* [33]. Fluid flow over a stretched cylinder using a dissipation was explored by Murthy *et al.,* [34] deploying magnetohydrodynamics as the boundary layer slip. Some more studies related to nano fluids are addressed by the authors [35-38].

As far as the authors are aware, no one has yet looked at the potential consequences of tangent hyperbolic fluid flow and heat transfer across a non-linearly stretched surface when a field of magnetism is present. The current investigation aims to build upon the findings of the prior research [39]. Nanofluid's heat flux and the boundary layer flow in presence of wall slip are the primary areas of investigation. The Keller-box technique serves to numerically solve the controlling partial equations once they are translated into ordinary differential equations.

2. Formulation

Considering a two-dimensional, incompressible, viscous, along with sustained boundary-level flow of tangential hyper nanofluid technology across a stretching surface at y = 0, which is stretching uniformly with speed $u_w = ax$. The stream is located at the area y > 0 where the field of magnets B_0^2, applied normally to the fluid. Since it is predicated that the Reynolds value is low, then magnetic field that is produced is minimal. The level of temperature near the boundary T_w, the nano particle fraction C_w are taken to be uniform at the stretched sheet. While y approaches infinitely, the ambient temperature nano particle fraction denotes as T_∞ and C_∞, respectively. The governing equations of the flow problem are [39-41]

$$\frac{\partial u}{\partial x}+\frac{\partial v}{\partial y}=0 \tag{1}$$

$$u\frac{\partial u}{\partial x}+v\frac{\partial u}{\partial y}=v(1-n)\frac{\partial^2 u}{\partial y^2}+\sqrt{2}\Gamma vn\frac{\partial u}{\partial y}\frac{\partial^2 u}{\partial y^2}-\frac{\sigma {B_0}^2 u}{\rho} \tag{2}$$

$$u\frac{\partial T}{\partial x}+v\frac{\partial T}{\partial y}=\alpha\frac{\partial^2 T}{\partial y^2}+\tau\left\{\mathrm{D_B}\frac{\partial C}{\partial y}\frac{\partial T}{\partial y}+\frac{\mathrm{D_T}}{T_\infty}\left(\frac{\partial T}{\partial y}\right)^2\right\} \tag{3}$$

$$u\frac{\partial C}{\partial x}+v\frac{\partial C}{\partial y}=\mathrm{D_B}\frac{\partial^2 C}{\partial y^2}+\frac{\mathrm{D_T}}{T_\infty}\frac{\partial^2 T}{\partial y^2} \tag{4}$$

The boundaries are provided by [41]

$$y=0\ \Rightarrow\begin{cases}u=u_w+U_{slip}\\ v=0\\ -k_f\frac{\partial T}{\partial y}=h_f\left(T_f-T\right)\\ C=C_w\end{cases},y\to\infty\Rightarrow\begin{cases}u\to 0\\ T\to T_\infty\\ C\to C_\infty\end{cases} \tag{5}$$

The velocity elements in the directions of x and y are denoted by u and v correspondingly. ν remains the viscosity kinematics, ρ represents the foundational flow density, Γ the constancy of time, n the Index of Power Law, T represents liquid's temperature, α diffusivity of temperature, c_p is particular temperature, τ denotes the proportion of flow thermal capacity to nanoparticles thermal capacity, $\mathrm{D_B}$ represents the Brownian motion parameter and $\mathrm{D_T}$ signifies a thermophoresis diffusing factor. Where C nanoparticles level, T_w and C_w represent concentrations and temperatures at the surface and T_∞ and C_∞ indicate the concentration of the nanoparticles and the ambient temperature, correspondingly.

In order to convert generalized problem equations as non-dimensional structure, the subsequent transforms are specified [39,41]

$$\eta=y\sqrt{\frac{a}{v}},\Psi=\sqrt{av}xf(\eta),u=axf'(\eta) \tag{6}$$

$$\theta(\eta)=\frac{\mathrm{T}-\mathrm{T}_\infty}{\mathrm{T}_f-\mathrm{T}_\infty},\phi(\eta)=\frac{C-C_\infty}{C_w-C_\infty}$$

where $u=\frac{\partial\Psi}{\partial y},v=-\frac{\partial\psi}{\partial x}$

Using Eq. (6) into Eq. (1) to Eq. (4), then we get the following ordinary equations

$$((1-n)+nWef'')f'''-f'^2+ff''-M^2f')=0 \tag{7}$$

$$\theta''+\Pr\left(f\theta'+Nb\phi'\theta'+Nt\theta'^2\right)=0 \tag{8}$$

$$\phi''+PrLef\phi'+\frac{Nt}{Nb}\theta''=0 \tag{9}$$

The boundary conditions are given by

$$\eta=0\Rightarrow\begin{cases}f'(0)=1+\lambda f''(0)\\ f(0)=0\\ \theta'(0)=-\gamma[1-\theta(0)]\\ \phi(0)=1\end{cases},\quad \eta\to\infty\Rightarrow\begin{cases}f'(\infty)\to 0\\ \theta=0\\ \phi=0\end{cases} \tag{10}$$

Where, $M=\frac{\sigma B_0^2}{a\rho}$, $Pr=\frac{v}{\alpha}$, $Nb=\frac{(\rho c)_p \mathrm{D_B}(C_w-C_\infty)}{(\rho c)_f v}$, $=\frac{\alpha}{\mathrm{D_B}}$, $Nt=\frac{(\rho c)_p \mathrm{D_T}(T_w-T_\infty)}{(\rho c)_f T_\infty v}$, $We=\Gamma x\sqrt{\frac{2a}{v^3}}$

$$\lambda=l\sqrt{\frac{a}{\vartheta}}\text{ and }\gamma=\frac{h_f}{k_f}\sqrt{\frac{\vartheta}{a}} \tag{11}$$

In the present steady, The Sherwood number, Nusselt number, and local skin friction are known by

$$\mathrm{C_{fx}}=\frac{\tau_w}{\frac{1}{2}\rho u_w^2},Nu_x=\frac{xq_w}{k(T_w-T_\infty)},Sh_x=\frac{xq_m}{\mathrm{D_B}(C_w-C_\infty)} \tag{12}$$

k represents thermal conductivity of the fluid and $\tau_w, q_w, q_m$are given by

$$\tau_w=\mu(1-n)\left[\frac{\partial u}{\partial y}\right]_{y=y_0}+\mu\frac{n\Gamma}{\sqrt{2}}\left[\frac{\partial u}{\partial y}\right]^3_{y=y_0},q_w=-k\left[\frac{\partial T}{\partial y}\right]_{y=y_0},q_m=-D_B\left[\frac{\partial C}{\partial y}\right]_{y=y_0} \tag{13}$$

Considering scaling parameters, then we get

$$\frac{Re_x^{1/2}C_{fx}}{2}=(1-n)f''(0)-\frac{nWe}{2}f''^3(0),Re_x^{1/2}Nu_x=-\theta'(0),Re_x^{1/2}Sh_x=-\phi'(0) \tag{14}$$

Where $\mathrm{Re_x}=xu_w/v$ Reynold number.

The Keller box program, which consists of the stages of finite difference approach, Newton's scheme, and block reduction procedure, explains the modified non-linear differential equations (9) to (11) using boundary constraints (12). Comparing this method to other popular strategies, this one appears to be the most adaptable and is currently using frequently. It can be described as being substantially faster, simpler to program, more effective, and simpler to use.

3. Numerical Solution

It is not feasible to obtain closed form solution because Eq. (9) to Eq. (11) are non-linear. The Keller-box technique, a finite difference approach, is applied in order to compute the

problem containing boundary circumstances computationally (12). To obtain numerical solutions, the following phases are the main components of the Keller-box technique

Step 1:

Applying the substitutions $f' = p, p' = q, \theta' = t, \phi' = g$

All of the ODEs must be transformed into 1st order ODEs in the early stages.

Step 2: Separation of domain

The rectangle grid in $x - \eta$ plane is deliberated in Figure 1, and the grid points are demarcated as:

$x^0 = 0, x^i = x^{i-1} + k_i,\ i = 1,2,3, \ldots \ldots I$

$\eta_0 = 0, \eta_j = \eta_{j-1} + h_i,\ j = 1,2,3, \ldots \ldots J$

Where (k_i, η_j) are the $\Delta x\ and\ \Delta\eta$ step length.

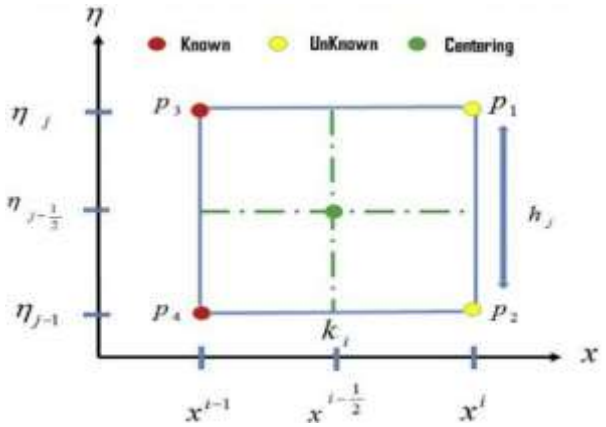

Fig. 1. Grid point labelling

Step 3: Newton's technique of linearization

As a consequence of Newton's method, the (i + 1)th iterations of the formulae may be found in the preceding equations

$()_j^{(i+1)} = ()_j^{(i)} + \delta()_j^{(i)}$

and after overlooking the higher-elevated bounds of $\delta()_j^{(i)}$ a linear tri-diagonal equation scheme.

Step 4: The bulk scheme and eliminating

The equation $F\delta = r$ has finally resulted in a bulk tri-diagonal matrix.

where

$$F=\begin{bmatrix} A1 & C1 & & & & \\ B2 & A2 & C2 & & & \\ \ddots & \ddots & \ddots & & & \\ & \ddots & \ddots & \ddots & & \\ & & B_{j-1} & A_{j-1} & C_{j-1} & \\ & & & B_j & A_j & \end{bmatrix},\ \delta=\begin{bmatrix} \delta_1 \\ \delta_2 \\ \vdots \\ \\ \vdots \\ \delta_{j-1} \\ \delta_j \end{bmatrix},\quad r=\begin{bmatrix} (r_1)_{j-\frac{1}{2}} \\ (r_2)_{j-\frac{1}{2}} \\ \vdots \\ \\ \vdots \\ (r_{j-1})_{j-\frac{1}{2}} \\ (r_j)_{j-\frac{1}{2}} \end{bmatrix}$$

where F is 7×7 block-sized matrix that corresponds to the size $J \times J$. However, $\delta \; and \; r$ are the vectors of order $J \times 1$. Now an efficient LU factorizing process is applied to solve for δ. In $F\delta = r$, F is splinted into lower and upper trigonal matrices, i.e. $F = LU$.

4. Results and Discussion

Using the procedure outlined in the preceding section, a numerical computing endeavor was undertaken to examine the outcomes for various measurements for the velocity slip, temperature slip, and magneto parameters (M). Displayed in Figure 2 to Figure 16 are the results of the parametric exploration. In order to ensure that the numerical scheme is accurate, we compare the current results for the skin friction coefficient, heat transfer coefficient, and mass transfer coefficient to the data in Table 1 to Table 3. In Table 1 we can see the skin friction coefficient as a function of the Hartmann number. We find that the skin friction coefficient decreases as the Hartmann number increases. The results are contrasted with the prior results and discovered to be in good agreement, which validates the numerical method. It is clear from Table 2 that skin friction coefficient improves as a function of power-law index, thermal slip, Wiesenberger number as well, Hartmann number, and velocity slip. The impacts of altering the settings with regard to Sherwood and Nusselt numbers are displayed in Table 3. Sherwood number is improved and Nusselt number is decreased by the Brownian motion parameter, Lewis number, and thermophoresis factor. While the Prandtl number causes to rise both the Nusselt number and Sherwood number.

Table 1
Comparing local skin friction coefficients with different Hartmann numbers

M	Hussain *et al.,* [43]	Akbar *et al.,* [42]	Khan *et al.,* [9]	Present $-C_f Re_x^{\frac{1}{2}}$
0	-1	-1	-1	-1
0.5	-1.1180	-1.11803	-1.11802	-1.11803
1.0	-1.4137	-1.41421	-1.41419	-1.41421
5	-2.4495	-2.44944	-2.44945	-2.449449
10	-3.3166	-3.31663	-3.31657	-3.31663
100	-10.0500	-10.04987	-10.04981	-10.0498
500	-22.3835	-22.38303	-22.38294	-22.38303
1000	-31.63859	-31.63859	-31.63851	-31.63859

Table 2
Variation of skin friction coefficient by varying $\lambda, \gamma, n, M, We$ values, for Pr=Le=0.0 and Nt=0.0, Nb=0.001

λ	γ	n	M	We	$-f''(0)$
0.0	0.0	0.0	0.0	0.5	1.0005
0.5	0.0	0.0	0.0	0.5	0.5452
1.0	0.5	0.0	0.0	0.5	0.3547
1.0	1.0	0.1	0.0	0.5	0.3761
1.0	1.0	0.2	0.5	0.5	0.4942
1.0	1.0	0.2	1.0	1.0	0.7298
1.0	1.0	0.2	1.0	1.5	0.7595

Table 3
Relationship between Sherwood and Nusselt numbers by varying $\lambda, \gamma, Pr, Nb, Nt, Le$ Values, for M = n = We = 0.0

λ	γ	Pr	Nb	Nt	Le	$-\theta'(0)$	$-\phi'(0)$
0.0	0.1	1.6	0.1	0.1	1.0	0.0661	0.7514
0.5	0.1	1.6	0.1	0.1	1.0	0.0540	0.6137
1.0	0.5	1.6	0.1	0.1	1.0	0.1694	0.4589
1.0	1.0	2.0	0.1	0.1	1.0	0.2817	0.4789
1.0	1.0	2.5	0.2	0.1	1.0	0.2730	0.6660
1.0	1.0	2.5	0.3	0.2	1.0	0.2281	0.6662
1.0	1.0	2.5	0.3	0.3	2.0	0.1949	1.0554
1.0	1.0	2.5	0.3	0.3	2.5	0.1887	1.2181

Figure 2 displays the velocity characteristics of the nanofluid as a function of slip variable λ and magnetic profile M. The trends in the profiles clearly show that when M is increased, the nanofluid velocity decreases, while the inverse trend holds true for λ. When electromagnetic force is divided by viscous force, the result is the magnetic field effect. Thus, the magnetic field acts as a barrier to the movement of the liquid. As one might expect, a drop in momentum occurs when the M is raised.

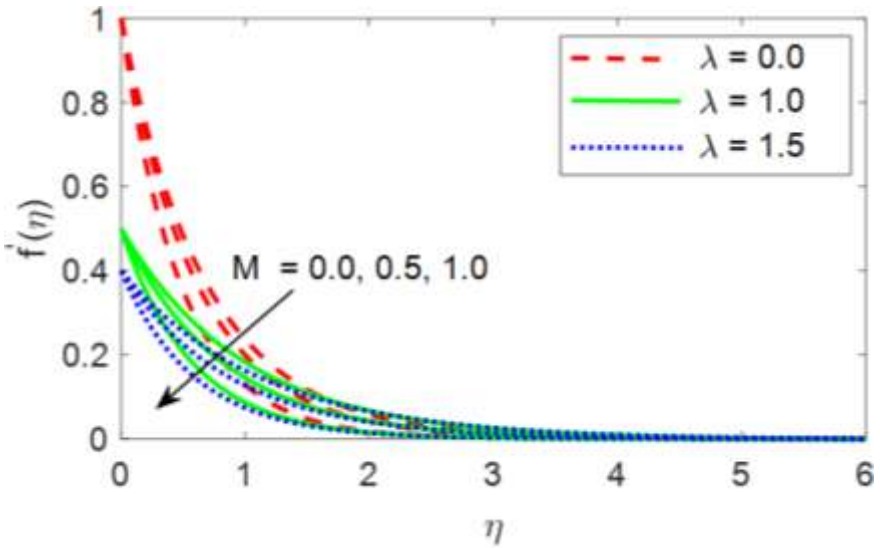

Fig. 2. Impact of M with λ on $f'(n)$

The profiles of the temperature distribution under the influence of the magnetic variable M and the thermo slip coefficient γ are shown in Figure 3. As both M and γ grow in value, it is clear that the temperature rises. This is because a larger value of the M causes the nanofluid's velocity to decrease, which in turn causes the temperature distribution to rise.

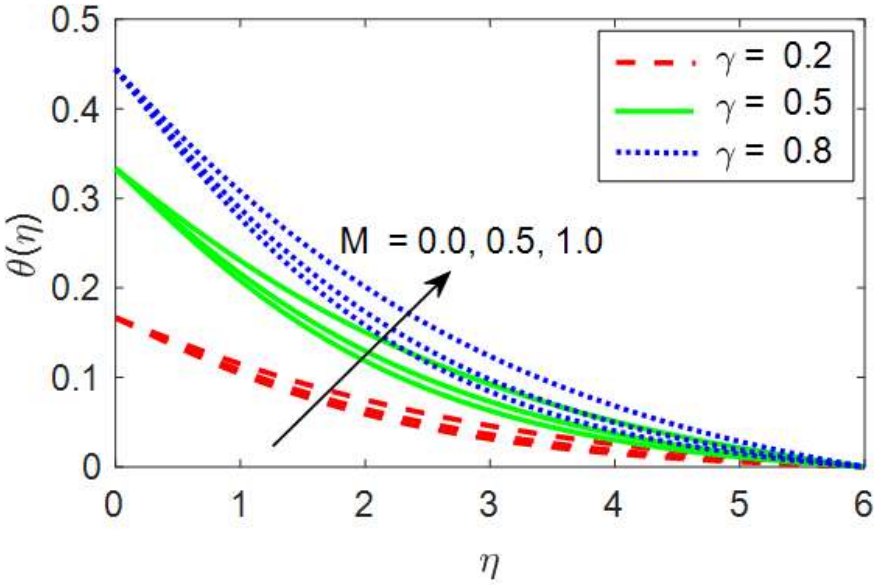

Fig. 3. Impact of M with γ on $\theta(n)$

The impact of the velocity slip component λ and Wiesenberger number We on the velocity profiles is apparent in the Figure 4. When the value of λ increases, the hydrodynamic boundary layer thins out and velocity decreases. The ratio of the fluid's relaxation time to a given process time is called the Wiesenberger number (We). When We increases, the flow velocity decreases and the hydrodynamic boundary level becomes thinner.

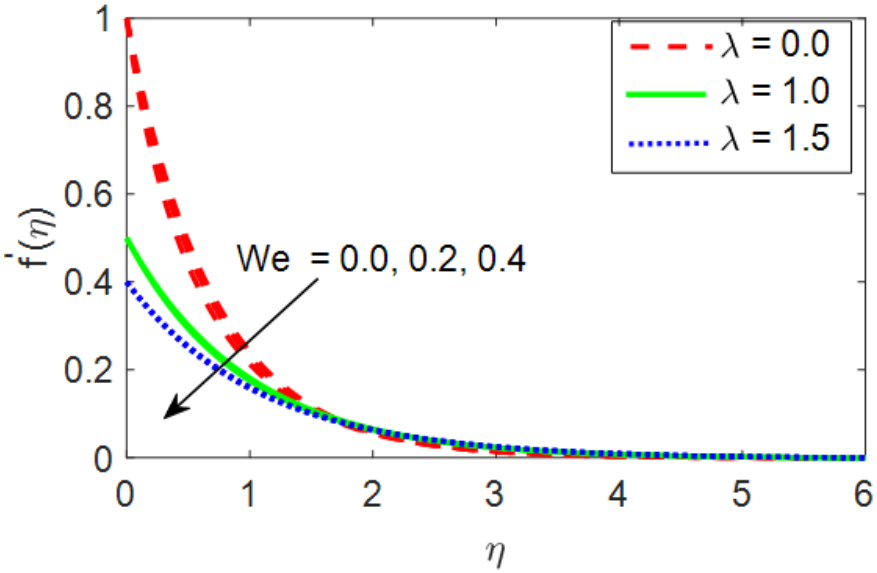

Fig. 4. Impact of We with λ on $f'(n)$

Figure 5 illustrates how the velocity profile is impacted by the velocity slip coefficient λ and a power law coefficient n. Looking at this graph, we can observe that as n and λ are larger, the velocity gets smaller. The lower the velocity, the bigger the value of λ, as seen in Figure 5. Actually, the fluid receives a portion of the stretching velocity as λ increases. Newtonian fluids (n = 0) and non-Newtonian fluids (n= 0.2, 0.5) both exhibit a drop in the velocity profile.

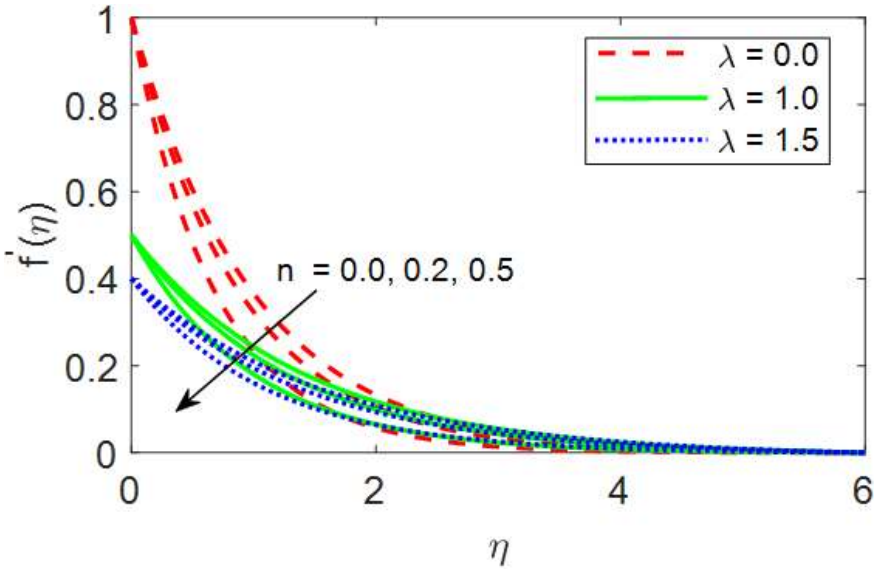

Fig. 5. Impact of n with λ on $f'(n)$

Both Figure 6 and Figure 7 show how the distributions of temperature and concentrations are affected through the thermal slip coefficient γ and the Brownian motion parameter Nb. Figure 6 illustrates how the thermal slip component affects the thermal field. As γ and Nb rise, the temperature field is noticed to rise as well as Brownian motion describes the irregular behavior of the nanomaterials in fluids. This chaotic motion quickens the collision between the nanoparticles and the liquid's particles, which causes the molecules' kinetic energy to be transformed to the thermal energy, resulting in temperatures to increase. Since heat is a source of energy for particles, Brownian motion is proportional to temperature. It follows that it rises as the temperature rises. As seen in Figure 7, which depicts that as γ, Nb rise, the concentration falls, and the concentration profile shows the same impact. It is due to the fact the collisions between the molecules in a solvent can induce the particles to move randomly and hence concentration is decreased.

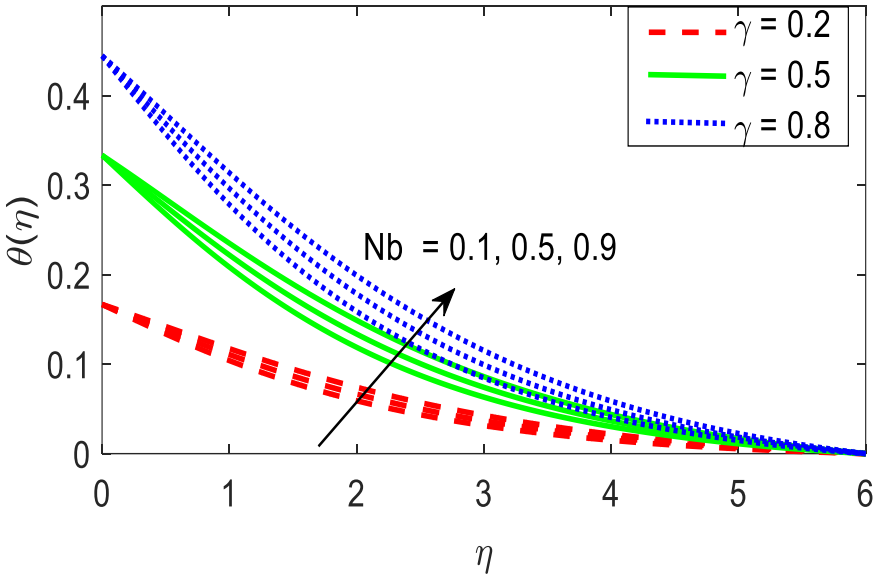

Fig. 6. Impact of Nb with γ on $\theta(n)$

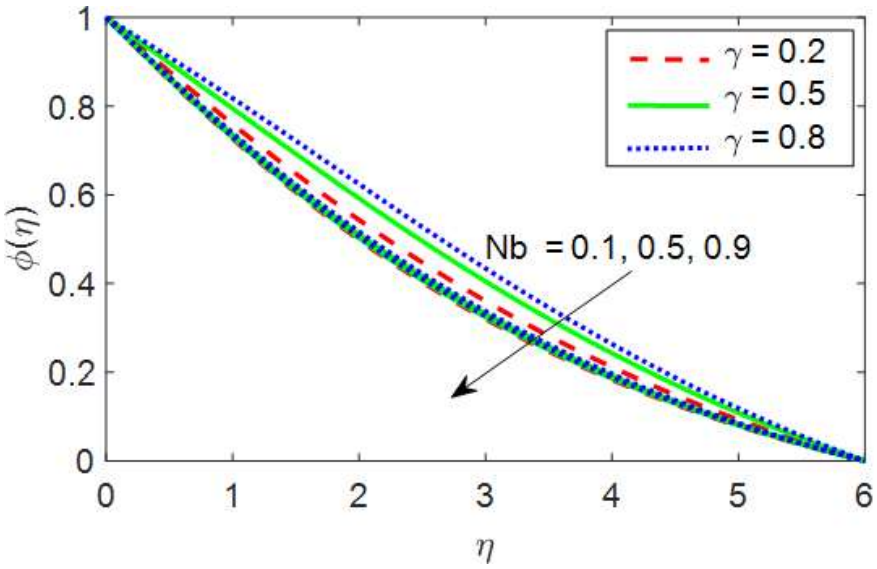

Fig. 7. Impact of Nb with γ on $\phi(n)$

Nanoparticles physically migrate from a warmer to a zone that is cooler due to the temperature differential; this process is known as thermophoresis. In Figure 8 and Figure 9, we can observe how the trends of concentrations as well as temperatures are impacted by the thermophoresis parameter Nt and the thermal slip parameter γ. The thermal and concentration boundary levels are found to be increased by a surge in Nt.

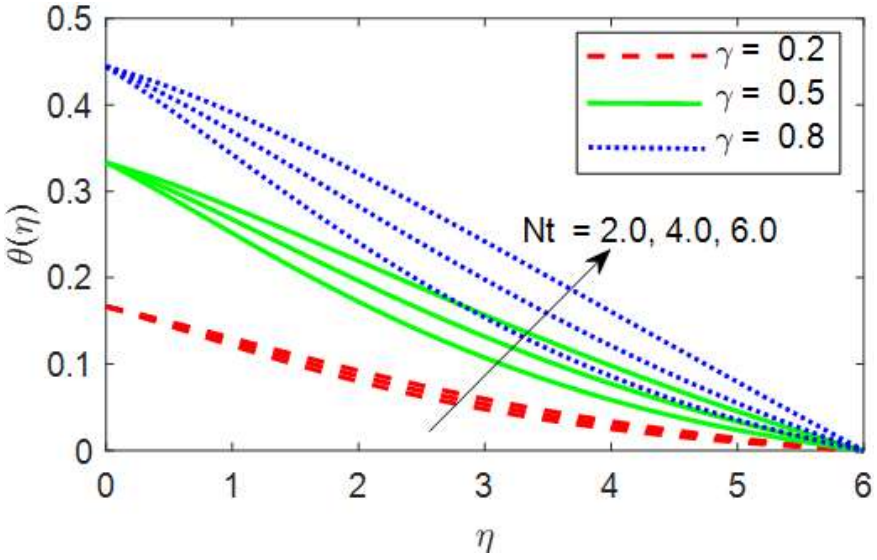

Fig. 8. Impact of Nt with γ on $\theta(n)$

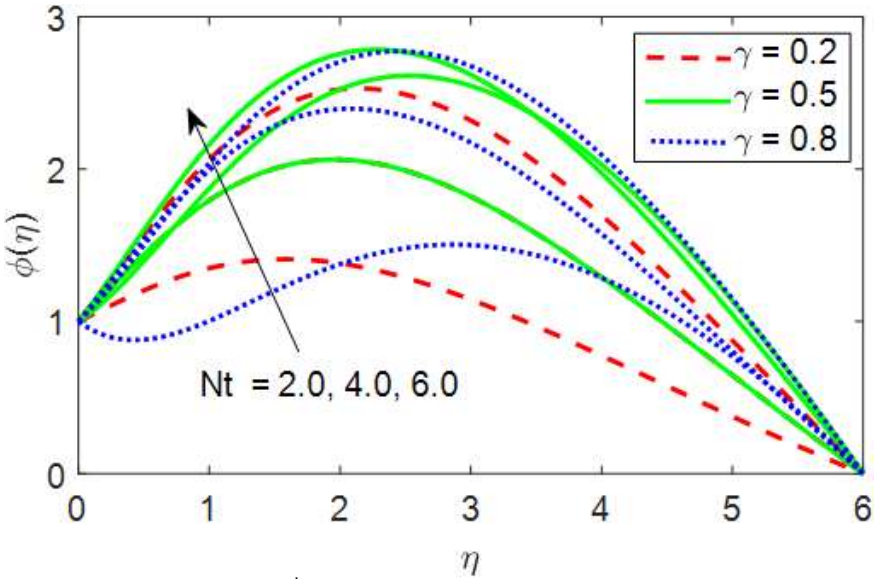

Fig. 9. Impact of Nt with γ on $\phi(n)$

Figure 10 shows how the temperature is affected by the velocity slip component λ, as well as the thermal slip component γ. At close range to the sheet, the temperature drops as the thermal slip parameter drops; however, beyond a certain distance g, this effect becomes blurry. As γ increases, the thermal transfer from the sheet to the fluid decreases, leading to a fall in temperature.

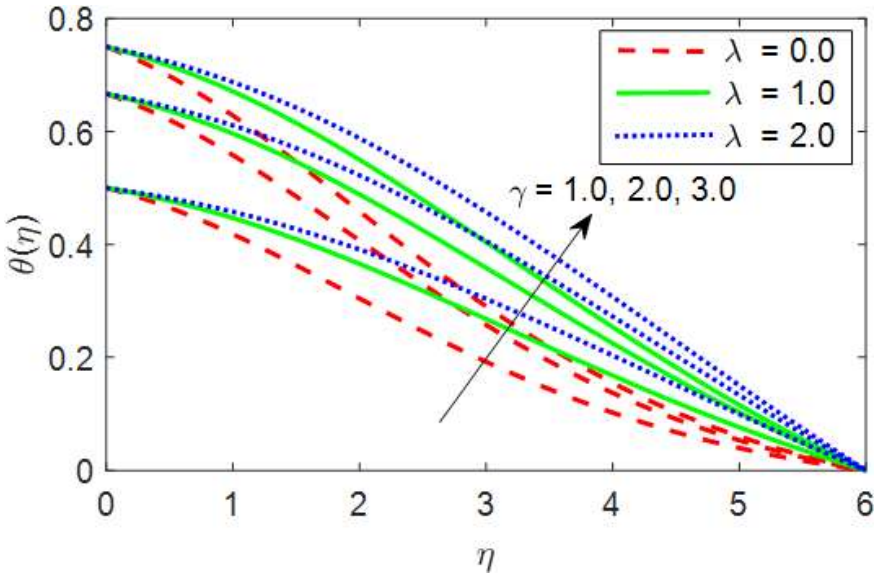

Fig. 10. Impact of γ with λ on $\theta(n)$

In Figure 11, we can see how three different values of the We and the magnetic parameters affect the skin friction as a function of the velocity slip component. When both the We and Magnetic numbers go up, the skin friction goes up as well. This is because as the Weissenberg number is elevated the polymer chains create elastic stresses, which can lead to greater drag and hence skin friction rises.

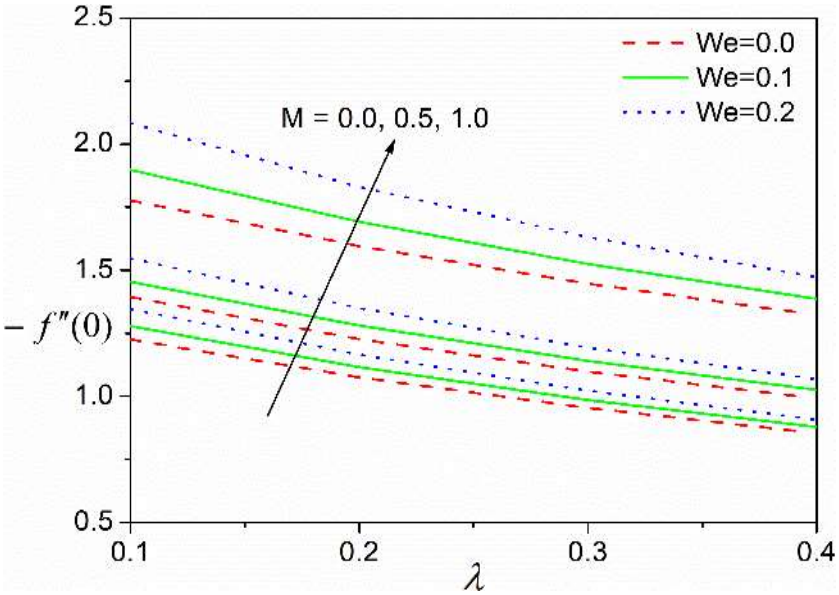

Fig. 11. Impact of M and We with λ on $-f''(0)$

Figure 12 shows the connection with the magnetic parameters' values, the power-lax index and the type of skin friction. The local skin friction number is found to rise as values for M and n increase. In the physical sense, magnetic fields have the ability to alter the motion of fluids via Lorentz forces, which, depending on the field's orientation and strength, may raise or lower the fluids' velocity. However, the rheological behavior of the fluid determines how the power law index impacts skin friction.

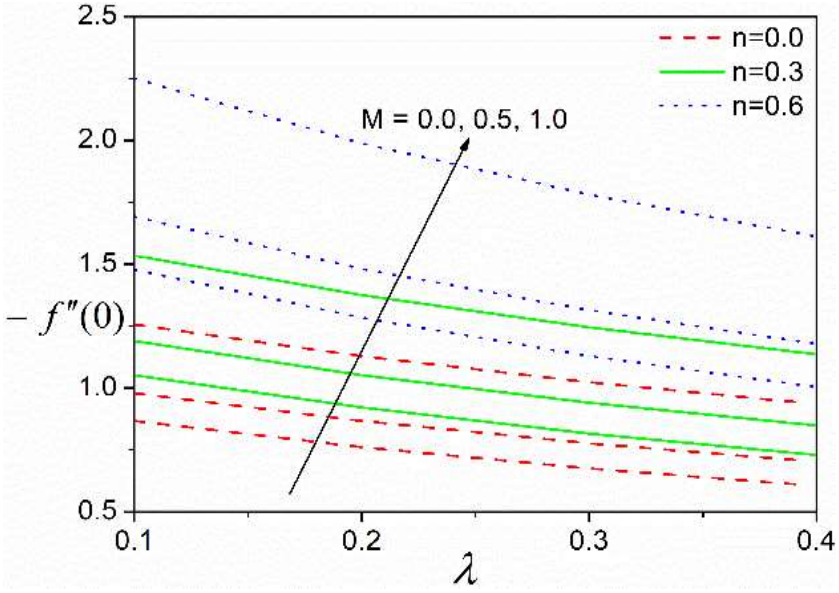

Fig. 12. Impact of M and n with λ on $-f''(0)$

Figure 13 to Figure 16 exhibit the consequences of the slip boundary condition on the Skin friction and Nusselt number for various values of the Brownian motion parameters, thermophoresis, and thermal slip.

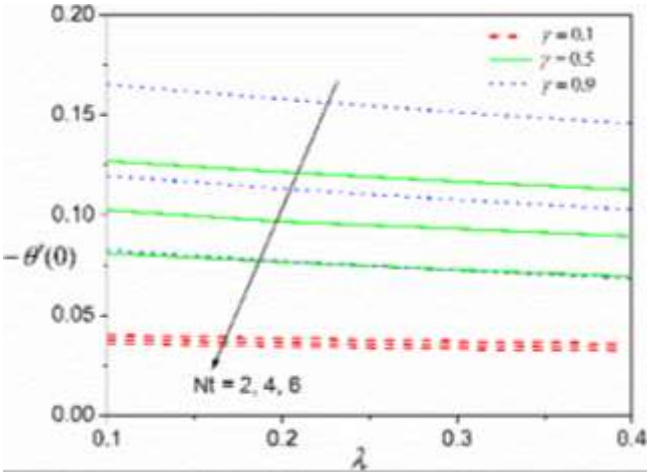

Fig. 13. Impact of Nt and γ with λ on $-\theta'(0)$

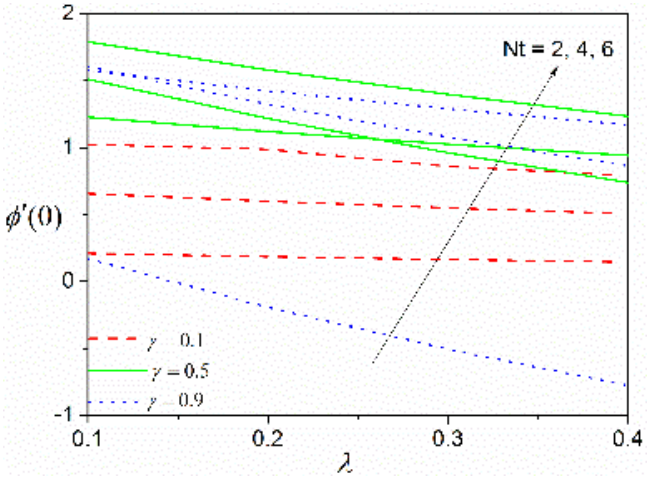

Fig. 14. Impact of Nt and γ with λ on $\phi'(0)$

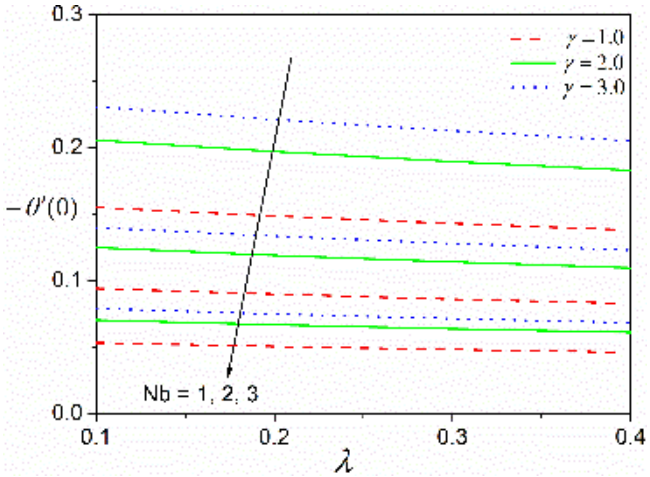

Fig. 15. Impact of Nb and γ with λ on $-\theta'(0)$

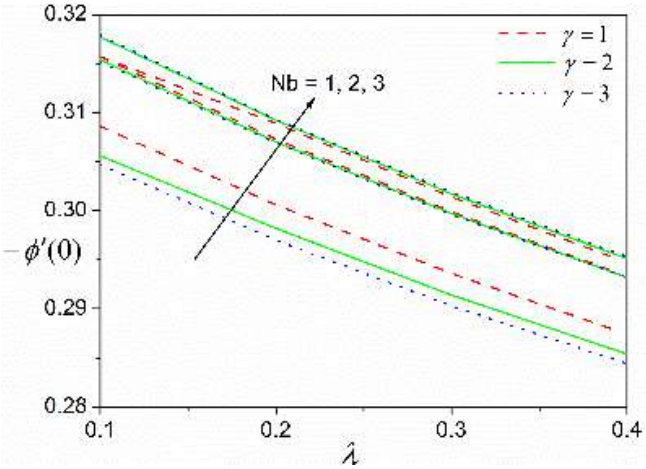

Fig. 16. Impact of Nb and γ with λ on $-\phi'(0)$

When the values of Nt, Nb, and γ are raised, the comparison of these figures reveals that the variation in the rates of dimensionless heat transport is reduced. Likewise, when the values of the thermophoresis Nt, the Brownian motion Nb, and the thermal slip variables vary, the mass transfer rate also increases. As the anisotropic slip (the difference between the two-directional slip velocities) and thermophoresis parameter are increased, While the mass transfer rate rises, the thermal transmission rate falls.

4. Conclusions

In this present investigation is focused on MHD hyperbolic tangent fluid flow of power law index with slip boundaries, considering magnetic variable M, Weissenberg parameter We, power-law index, Brownian motion and Thermophoresis parameters Nb and Nt. Keller box technique is used for solving the problem and the outcomes of the investigation is summarized below

i. The magnetic component induces that the temperature increases and velocity profile decrease.
ii. For higher values of the power-law index, Weissenberg parameter and the velocity slip variable, lower the velocity and hence thinning of hydro dynamic boundary layer.
iii. Thermal slip ensures raise the temperature.
iv. The effect of Brownian motion component Nb is to raise the fluid's temperature while lowering its concentration.
v. Thermophoresis parameter Nt enhances then we can observe increment in the thermal and concentration boundary layer.
vi. Weissenberg number and power-law index raise Skin friction.
vii. For the higher amount of Nt, Nb, Gamma, reduces the mass transport and rate of thermal transmission.

Incorporating thermal factors, such as changing thermal conductivity, internal heat generation/absorption, and thermal radiation, is within the purview of future work for the current study. More thorough understanding could be gained by investigating the flow's response to both thermal and magnetic fields simultaneously.

Acknowledgements
The authors would like to express their gratitude to the editor for all of his helpful suggestions during the editing process. Our work has been greatly enhanced in terms of clarity and rigor thanks to the anonymous reviewers with insightful remarks and suggestions. Their knowledge and care for detail are major reasons why this work is of such high quality.

References

[1] Hady, Fekry M., Fouad S. Ibrahim, Sahar M. Abdel-Gaied, and Mohamed R. Eid. "Radiation effect on viscous flow of a nanofluid and heat transfer over a nonlinearly stretching sheet." *Nanoscale Research Letters* 7, no. 1 (2012): 229. https://doi.org/10.1186/1556-276X-7-229

[2] Sakiadis, Byron C. "Boundary-layer behavior on continuous solid surfaces: I. Boundary-layer equations for two-dimensional and axisymmetric flow." *AIChE Journal* 7, no. 1 (1961): 26-28. https://doi.org/10.1002/aic.690070108

[3] Cortell, R. "Flow of a viscous fluid over a non-linearly (quadratic) porous stretching surface." In *Proceedings of the International Conference on Future Information Technology and Management Science & Engineering*, p. 14. 2012.

[4] Rashidi, Mohammad Mehdi, Behnam Rostami, Navid Freidoonimehr, and Saeid Abbasbandy. "Free convective heat and mass transfer for MHD fluid flow over a permeable vertical stretching sheet in the presence of the radiation and buoyancy effects." *Ain Shams Engineering Journal* 5, no. 3 (2014): 901-912. https://doi.org/10.1016/j.asej.2014.02.007

[5] Raptis, A., and C. Perdikis. "Viscous flow over a non-linearly stretching sheet in the presence of a chemical reaction and magnetic field." *International Journal of Non-Linear Mechanics* 41, no. 4 (2006): 527-529. https://doi.org/10.1016/j.ijnonlinmec.2005.12.003

[6] Hayat, T., Z. Abbas, and T. Javed. "Mixed convection flow of a micropolar fluid over a non-linearly stretching sheet." *Physics Letters A* 372, no. 5 (2008): 637-647. https://doi.org/10.1016/j.physleta.2007.08.006

[7] Khan, Ansab Azam, Khairy Zaimi, Suliadi Firdaus Sufahani, and Mohammad Ferdows. "MHD flow and heat transfer of double stratified micropolar fluid over a vertical permeable shrinking/stretching sheet with chemical reaction and heat source." *Journal of Advanced Research in Applied Sciences and Engineering Technology* 21, no. 1 (2020): 1-14. https://doi.org/10.37934/araset.21.1.114

[8] Prasad, K. V., K. Vajravelu, and P. S. Datti. "The effects of variable fluid properties on the hydro-magnetic flow and heat transfer over a non-linearly stretching sheet." *International Journal of Thermal Sciences* 49, no. 3 (2010): 603-610. https://doi.org/10.1016/j.ijthermalsci.2009.08.005

[9] Khan, Umar, Naveed Ahmed, Sheikh Irfan Ullah Khan, and Syed Tauseef Mohyud-din. "Thermo-diffusion effects on MHD stagnation point flow towards a stretching sheet in a nanofluid." *Propulsion and Power Research* 3, no. 3 (2014): 151-158. https://doi.org/10.1016/j.jppr.2014.07.006

[10] Rasool, Ghulam, Anum Shafiq, Marei S. Alqarni, Abderrahim Wakif, Ilyas Khan, and Muhammad Shoaib Bhutta. "Numerical scrutinization of Darcy-Forchheimer relation in convective magnetohydrodynamic nanofluid flow bounded by nonlinear stretching surface in the perspective of heat and mass transfer." *Micromachines* 12, no. 4 (2021): 374. https://doi.org/10.3390/mi12040374

[11] Idowu, A. S., and B. O. Falodun. "Effects of thermophoresis, Soret-Dufour on heat and mass transfer flow of magnetohydrodynamics non-Newtonian nanofluid over an inclined plate." *Arab Journal of Basic and Applied Sciences* 27, no. 1 (2020): 149-165. https://doi.org/10.1080/25765299.2020.1746017

[12] Naz, Rahila, Muhamamd Sohail, Memoona Bibi, and Maryiam Javed. "Numerical treatment of magneto hydrodynamic Carreau liquid with heat and mass transport containing gyrotactic microorganisms." *Scientia Iranica* 30, no. 6 (2023): 2223-2234.

[13] Uddin, Md Jashim, W. A. Khan, and Ahmad Izani Ismail. "Lie group analysis and numerical solutions for magnetoconvective slip flow along a moving chemically reacting radiating plate in porous media with variable mass diffusivity." *Heat Transfer-Asian Research* 45, no. 3 (2016): 239-263. https://doi.org/10.1002/htj.21161

[14] Nadeem, Sohail, and Noreen Sher Akbar. "Series solutions for the peristaltic flow of a Tangent hyperbolic fluid in a uniform inclined tube." *Zeitschrift Für Naturforschung A* 65, no. 11 (2010): 887-895. https://doi.org/10.1515/zna-2010-1101

[15] Malik, M. Y., T. Salahuddin, Arif Hussain, and S. Bilal. "MHD flow of tangent hyperbolic fluid over a stretching cylinder: using Keller box method." *Journal of Magnetism and Magnetic Materials* 395 (2015): 271-276. https://doi.org/10.1016/j.jmmm.2015.07.097

[16] Naseer, Muhammad, Muhammad Yousaf Malik, Sohail Nadeem, and Abdul Rehman. "The boundary layer flow of hyperbolic tangent fluid over a vertical exponentially stretching cylinder." *Alexandria Engineering Journal* 53, no. 3 (2014): 747-750. https://doi.org/10.1016/j.aej.2014.05.001

[17] Salahuddin, T., Imad Khan, M. Y. Malik, Mair Khan, Arif Hussain, and Muhammad Awais. "Internal friction between fluid particles of MHD tangent hyperbolic fluid with heat generation: Using coefficients improved by Cash and Karp." *European Physical Journal Plus* 132, no. 5 (2017): 205. https://doi.org/10.1140/epjp/i2017-11477-9
[18] Salahuddin, T., M. Y. Malik, Arif Hussain, Muhammad Awais, Imad Khan, and Mair Khan. "Analysis of tangent hyperbolic nanofluid impinging on a stretching cylinder near the stagnation point." *Results in Physics* 7 (2017): 426-434. https://doi.org/10.1016/j.rinp.2016.12.033
[19] Hussain, Arif, M. Y. Malik, T. Salahuddin, A. Rubab, and Mair Khan. "Effects of viscous dissipation on MHD tangent hyperbolic fluid over a nonlinear stretching sheet with convective boundary conditions." *Results in Physics* 7 (2017): 3502-3509. https://doi.org/10.1016/j.rinp.2017.08.026
[20] Nadeem, S., Sadaf Ashiq, Noreen Sher Akbar, and Changhoon Lee. "Peristaltic flow of hyperbolic tangent fluid in a diverging tube with heat and mass transfer." *Journal of Energy Engineering* 139, no. 2 (2013): 124-135. https://doi.org/10.1061/(ASCE)EY.1943-7897.0000094
[21] Khan, Mair, Arif Hussain, M. Y. Malik, T. Salahuddin, and Farzana Khan. "Boundary layer flow of MHD tangent hyperbolic nanofluid over a stretching sheet: a numerical investigation." *Results in Physics* 7 (2017): 2837-2844. https://doi.org/10.1016/j.rinp.2017.07.061
[22] Bartwal, Priya, Himanshu Upreti, Alok Kumar Pandey, Navneet Joshi, and B. P. Joshi. "Application of modified Fourier's law in a fuzzy environment to explore the tangent hyperbolic fluid flow over a non-flat stretched sheet using the LWCM approach." *International Communications in Heat and Mass Transfer* 153 (2024): 107332. https://doi.org/10.1016/j.icheatmasstransfer.2024.107332
[23] Athal, I., Byeon Haewon, A. Sasikala, B. Narsimha Reddy, Vediyappan Govindan, P. Maddileti, K. Saritha et al. "Combined impact of radiation and chemical reaction on MHD hyperbolic tangent nanofluid boundary layer flow past a stretching sheet." *Modern Physics Letters B* 38, no. 16 (2024): 2341010. https://doi.org/10.1142/S0217984923410105
[24] Mustafa, M., S. Hina, T. Hayat, and A. Alsaedi. "Slip effects on the peristaltic motion of nanofluid in a channel with wall properties." *Journal of Heat Transfer* 135, no. 4 (2013): 041701. https://doi.org/10.1115/1.4023038
[25] Mukhopadhyay, Swati. "Slip effects on MHD boundary layer flow over an exponentially stretching sheet with suction/blowing and thermal radiation." *Ain Shams Engineering Journal* 4, no. 3 (2013): 485-491. https://doi.org/10.1016/j.asej.2012.10.007
[26] Malvandi, A., F. Hedayati, and D. D. Ganji. "Slip effects on unsteady stagnation point flow of a nanofluid over a stretching sheet." *Powder Technology* 253 (2014): 377-384. https://doi.org/10.1016/j.powtec.2013.11.049
[27] Ibrahim, Wubshet, and Bandari Shankar. "MHD boundary layer flow and heat transfer of a nanofluid past a permeable stretching sheet with velocity, thermal and solutal slip boundary conditions." *Computers & Fluids* 75 (2013): 1-10. https://doi.org/10.1016/j.compfluid.2013.01.014
[28] Singh, Khilap, Alok Kumar Pandey, and Manoj Kumar. "Numerical approach for chemical reaction and suction/injection impacts on magnetic micropolar fluid flow through porous wedge with Hall and ion-slip using Keller Box method." *Waves in Random and Complex Media* (2021): 1-26. https://doi.org/10.1080/17455030.2021.1988757
[29] Turkyilmazoglu, M. "Dual and triple solutions for MHD slip flow of non-Newtonian fluid over a shrinking surface." *Computers & Fluids* 70 (2012): 53-58. https://doi.org/10.1016/j.compfluid.2012.01.009
[30] Ellahi, Rahmat, Sultan Z. Alamri, Abdul Basit, and A. Majeed. "Effects of MHD and slip on heat transfer boundary layer flow over a moving plate based on specific entropy generation." *Journal of Taibah University for Science* 12, no. 4 (2018): 476-482. https://doi.org/10.1080/16583655.2018.1483795
[31] Reddy, P. BalaAnki, S. Suneetha, and N. Bhaskar Reddy. "Numerical study of magnetohydrodynamics (MHD) boundary layer slip flow of a Maxwell nanofluid over an exponentially stretching surface with convective boundary condition." *Propulsion and Power Research* 6, no. 4 (2017): 259-268. https://doi.org/10.1016/j.jppr.2017.11.002
[32] Aly, Emad H., and Hamed M. Sayed. "Magnetohydrodynamic and thermal radiation effects on the boundary-layer flow due to a moving extensible surface with the velocity slip model: A comparative study of four nanofluids." *Journal of Magnetism and Magnetic Materials* 422 (2017): 440-451. https://doi.org/10.1016/j.jmmm.2016.08.072
[33] Reddy, Y. Dharmendar, Fateh Mebarek-Oudina, B. Shankar Goud, and A. I. Ismail. "Radiation, velocity and thermal slips effect toward MHD boundary layer flow through heat and mass transport of Williamson nanofluid with porous medium." *Arabian Journal for Science and Engineering* 47, no. 12 (2022): 16355-16369. https://doi.org/10.1007/s13369-022-06825-2
[34] Murthy, M. Krishna, Chakravarthula S. K. Raju, V. Nagendramma, Sabir Ali Shehzad, and Ali Jawad Chamkha. "Magnetohydrodynamics boundary layer slip Casson fluid flow over a dissipated stretched cylinder." In *Defect and Diffusion Forum*, vol. 393, pp. 73-82. Trans Tech Publications Ltd, 2019. https://doi.org/10.4028/www.scientific.net/DDF.393.73

[35] Upreti, Himanshu, Alok Kumar Pandey, Tanya Gupta, and Subrahamanyam Upadhyay. "Exploring the nanoparticle's shape effect on boundary layer flow of hybrid nanofluid over a thin needle with quadratic Boussinesq approximation: Legendre wavelet approach." *Journal of Thermal Analysis and Calorimetry* 148, no. 22 (2023): 12669-12686. https://doi.org/10.1007/s10973-023-12502-9

[36] Chintalapudi, Ravikiran, Halesh Koti, B. Shashidar Reddy, and K. Saritha. "Mechanisms of Diffusion thermo and Thermal diffusion on MHD Mixed Convection Flow of Casson fluid over a vertical cone with porous material in the presence of thermophoresis and a Brownian motion." *Journal of Advanced Research in Numerical Heat Transfer* 17, no. 1 (2024): 29-43. https://doi.org/10.37934/arnht.17.1.2943

[37] Upreti, Himanshu, Alok Kumar Pandey, Manoj Kumar, and O. D. Makinde. "Darcy-Forchheimer flow of CNTs-H_2O nanofluid over a porous stretchable surface with Xue model." *International Journal of Modern Physics B* 37, no. 02 (2023): 2350018. https://doi.org/10.1142/S0217979223500182

[38] Upreti, Himanshu, Alok Kumar Pandey, Navneet Joshi, and O. D. Makinde. "Thermodynamics and heat transfer analysis of magnetized Casson hybrid nanofluid flow via a Riga plate with thermal radiation." *Journal of Computational Biophysics and Chemistry* 22, no. 03 (2023): 321-334. https://doi.org/10.1142/S2737416523400070

[39] Akbar, Noreen Sher, S. Nadeem, R. Ul Haq, and Z. H. Khan. "Numerical solutions of magnetohydrodynamic boundary layer flow of tangent hyperbolic fluid towards a stretching sheet." *Indian Journal of Physics* 87 (2013): 1121-1124. https://doi.org/10.1007/s12648-013-0339-8

[40] Khan, W. A., and I. Pop. "Boundary-layer flow of a nanofluid past a stretching sheet." *International Journal of Heat and Mass Transfer* 53, no. 11-12 (2010): 2477-2483. https://doi.org/10.1016/j.ijheatmasstransfer.2010.01.032

[41] Kuznetsov, A. V., and D. A. Nield. "Natural convective boundary-layer flow of a nanofluid past a vertical plate." *International Journal of Thermal Sciences* 49, no. 2 (2010): 243-247. https://doi.org/10.1016/j.ijthermalsci.2009.07.015

[42] Akbar, Noreen Sher, Abdelhalim Ebaid, and Z. H. Khan. "Numerical analysis of magnetic field effects on Eyring-Powell fluid flow towards a stretching sheet." *Journal of Magnetism and Magnetic Materials* 382 (2015): 355-358. https://doi.org/10.1016/j.jmmm.2015.01.088

[43] Hussain, Arif, M. Y. Malik, M. Awais, T. Salahuddin, and S. Bilal. "Computational and physical aspects of MHD Prandtl-Eyring fluid flow analysis over a stretching sheet." *Neural Computing and Applications* 31 (2019): 425-433. https://doi.org/10.1007/s00521-017-3017-5